

## Echo spectroscopy of Anderson localization

T. Micklitz<sup>1</sup>, C. A. Müller<sup>2,3</sup>, and A. Altland<sup>4</sup>

<sup>1</sup>*Centro Brasileiro de Pesquisas Físicas, Rua Xavier Sigaud 150, 22290-180, Rio de Janeiro, Brazil*

<sup>2</sup>*Fachbereich Physik, Universität Konstanz, 78457 Konstanz, Germany*

<sup>3</sup>*Laboratoire Kastler-Brossel, Université Pierre et Marie Curie-Paris 6, ENS, CNRS, 75005 Paris, France*

<sup>4</sup>*Institut für Theoretische Physik, Universität zu Köln, Zùlpicher Str. 77, 50937 Köln, Germany*

(Dated: June 27, 2014)

We propose a conceptually new framework to study the onset of Anderson localization in disordered systems. The idea is to expose waves propagating in a random scattering environment to a sequence of short dephasing pulses. The system responds through coherence peaks forming at specific echo times, each echo representing a particular process of quantum interference. We suggest a concrete realization for cold gases, where quantum interferences are observed in the momentum distribution of matter waves in a laser speckle potential. This defines a challenging, but arguably realistic framework promising to yield unprecedented insight into the mechanisms of Anderson localization.

PACS numbers: 71.15.Rn, 42.25.Dd, 03.75.-b, 05.60Gg

Coherent quantum wave scattering is a salient feature of disordered or chaotic quantum systems. Its manifestations range from coherence peaks in scattering cross sections over weak localization and quantum fluctuation phenomena in metals, to strong (Anderson) localization [1]. Phenomena of this type have been observed with light [2] or microwaves [3], in electronic conductors [4], with cold atomic gases [5–8], photonic crystals [9], and classical waves [10]. Semiclassically, quantum coherence is understood in terms of the interference of Feynman path amplitudes. Quantum effects arise when classically distinct amplitudes interfere to yield non-classical contributions to physical observables, see Fig. 1. For instance, coherent backscattering (CBS) and weak localization [11] are due to the interference of mutually time reversed paths. Similarly, coherent forward scattering is caused by the concatenation of two such processes, or again by the interference of two self retracing loops traversed in different order [12, 13], etc. Quantum coherent contributions are often discriminated from classical background contributions by their strong sensitivity to dephasing and decoherence. However, other than suppressing coherence, generic sources of decoherence – external magnetic fields, AC electromagnetic radiation, etc. – do not provide much insight into the mechanisms of quantum interference in disordered media. Furthermore, decoherence often acts as a source of heating (it certainly does so on the temperature scales relevant to cold atomic gases) and leads to an unwelcome nonequilibrium shakeup of the system.

In this paper, we suggest an alternative protocol for probing quantum coherence. Its advantage is that it offers much more specific information and at the same time is less intrusive than persistent external irradiation. The idea is to expose the quantum system to a source of decoherence only at specific ‘signal times’,  $t_1, t_2, \dots$ . The system then responds to this perturbation at ‘echo times’  $\tau_1, \tau_2, \dots$ , which are in well-defined correspondence to

the signal times. Each of these echoes corresponds to a specific mechanism of quantum-coherent scattering. For example, an echo at time  $2t_1$  after a decoherence pulse applied at time  $t_1$  is a tell-tale signature of the CBS effect, cf. Fig. 1c). Likewise, an echo observed at time  $2(t_2 - t_1)$  in response to *two* pulses at  $t_1$  and  $t_2 > 2t_1$  identifies a contribution to forward scattering coherence, etc. The observation of a temporal echo pattern thus realizes a highly resolved probe of quantum coherence in random scattering media. In the following, we introduce

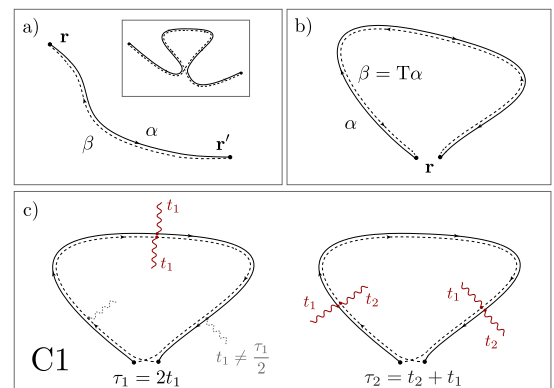


FIG. 1: a) Copropagating Feynman paths,  $\alpha = \beta$ , yield the classical contribution to the two-point transition probability  $\mathbf{r} \rightarrow \mathbf{r}'$  (we use the convention where the particle/hole propagates with/against the direction of the arrow). Inset: weak localization loop. b) Coherent contribution,  $\beta = T\alpha$  to return probability  $\mathbf{r} \rightarrow \mathbf{r}$ , where  $T\alpha$  is the time reverse of  $\alpha$ . c) Coherent backscattering contribution in the presence of dephasing pulses (wiggly lines). While a pulse acting at generic traversal times  $t_1 \neq T/2$  (dashed wiggly lines) suppresses phase coherence, a pulse at  $t_1 = T/2$  affects particle and hole amplitudes in synchronicity and does not reduce their coherence. Right: synchronicity condition for a bi-temporal pulse acting at  $t_1, t_2$  is realized for traversal times  $T = t_1 + t_2$ , and a coherence signal will be observed at this time.

the principles of coherent echo response in general terms. We will then specialize to a system of observables relevant to cold atom scattering experiments [14, 15], which offer a degree of control required for the observation of the CBS echo, and possibly higher-order coherence echoes.

*Feynman path approach to coherence echoes:*—Consider the retarded quantum correlation function

$$X \equiv \left\langle \hat{O}_{\mathbf{x}}(t) \hat{O}_{\mathbf{x}'}(0) \right\rangle, \quad (1)$$

where the brackets stand for an average over quantum and disorder distributions,  $O_{\mathbf{x}} = |\mathbf{x}\rangle\langle\mathbf{x}|$  is a projector onto a squeezed state defined by  $\langle\mathbf{r}'|\mathbf{x}\rangle = \frac{1}{(2\pi)^{d/4}} \frac{1}{(\Delta r)^{d/2}} \exp\left(-\frac{(\mathbf{r}'-\mathbf{r})^2}{(2\Delta r)^2} + \frac{i}{\hbar}\mathbf{p}\cdot\mathbf{r}'\right)$ , the scale  $\Delta r$  sets the spatial resolution of the operator, and  $\mathbf{x} = (\mathbf{r}, \mathbf{p})$  is a phase space vector comprising real space ( $\mathbf{r}$ ) and momentum space ( $\mathbf{p}$ ) coordinates. In the limit of infinitely sharp resolution  $\hat{O}_{\mathbf{x}} \xrightarrow{\Delta r \rightarrow 0} |\mathbf{r}\rangle\langle\mathbf{r}|$  projects onto real-space coordinates, and the correlation function (1) may serve, e.g., as a building block for a point-contact transport observable. In the opposite limit  $\hat{O}_{\mathbf{x}} \xrightarrow{\Delta r \rightarrow \infty} |\mathbf{p}\rangle\langle\mathbf{p}|$  projects onto momentum coordinates, and the correlation function relates to the cross section for the scattering process  $\mathbf{p} \rightarrow \mathbf{p}'$ . Intermediate values of  $\Delta r$  probe transitions between coherent-state-like wave packets of minimal quantum uncertainty centered around  $\mathbf{x}$ .

To introduce the concept of coherence echoes, we consider first the case  $\Delta r = 0$  of a space-local two point correlation function. Within a Feynman path approach the expectation value (1) then assumes the form

$$X = \sum_{\alpha, \beta} \left\langle e^{\frac{i}{\hbar}(S[\alpha] - S[\beta])} M_{\alpha\beta} \right\rangle, \quad (2)$$

where  $\alpha, \beta$  are paths connecting  $\mathbf{r}$  and  $\mathbf{r}'$  in time  $t$ ,  $S[\alpha]$  is the corresponding classical action, and  $M_{\alpha\beta}$  is a container symbol for matrix elements and semiclassical stability amplitudes. The double sum is dominated by path configurations of nearly identical action  $|S[\alpha] - S[\beta]| \lesssim \hbar$ , all other contributions are effectively averaged out by large phase fluctuations. The set of contributing paths includes  $\alpha = \beta$  [Fig. 1a)], which yields the classical, phase-insensitive approximation  $X_0$  of the observable (2). Generic quantum corrections ('weak localization corrections') are due to the branching and subsequent re-unification of path segments to a phase coherent entity [Fig. 1a) inset]. Such processes, which at large time/length scales may accumulate to drive a system into an Anderson localized phase, renormalize the system's effective diffusivity and are not central to our present approach. Coherence signals probed by echoes arise when the two observation points  $\mathbf{r} \rightarrow \mathbf{r}'$  approach each other [Fig. 1b)]. In this case, the double sum is dominated by the classical contribution  $\alpha = \beta$ , and an *equally strong* quantum contribution  $\beta = T\alpha$ , where  $T\alpha$  is the

time reversed of the path  $\beta$  [Fig. 1b)] [16]. Consider now a single external radiation pulse applied to the system at time  $t_1 > 0$  [Fig. 1c)]. At  $t_1$  a particle propagating along  $\alpha$  is at coordinate  $\mathbf{r}(t_1)$ , while a particle propagating along  $T\alpha$  is at  $\mathbf{r}(T - t_1)$ , where  $T$  is the loop traversal time. In general, these coordinates differ from each other, which means that the external pulse affects the quantum phases carried by the two amplitudes in different ways—causing decoherence. However, if the traversal time is such that  $t_1 = T/2$ , then  $\mathbf{r}(t_1) = \mathbf{r}(T - t_1)$ , and coherence is briefly regained [17]. An observation of the system at time  $t = 2t_1 \equiv \tau_1$  probes path pairs of just this 'resonant' length, which can be witnessed by the formation of a coherence peak in the observable  $X$ .

*Perturbed quantum diffusion:*—To obtain a quantitative understanding of the echo signal, we consider a weakly disordered medium in which the paths entering individual segments of pair propagation (the double lines in Fig. 1) describe diffusion. For fixed initial and final coordinates  $\mathbf{r}$  and  $\mathbf{r}'$  and propagation time  $t$ , the sum over all co-propagating paths is described by a classical diffusion propagator  $\Pi_D(\mathbf{r}, \mathbf{r}'; t)$ , or 'diffuson' for brevity. The diffuson solves the diffusion equation  $(\partial_t - D\partial_{\mathbf{r}}^2)\Pi_D(\mathbf{r}, \mathbf{r}'; t) = \delta(\mathbf{r} - \mathbf{r}')\delta(t)$ , where  $D = v^2\tau/d$  is the classical diffusion coefficient,  $\tau$  the elastic scattering time, and  $v = |\mathbf{p}|/m$  the velocity of particles of mass  $m$ . Likewise, the sum over all contributions to a segment  $\mathbf{r} \rightarrow \mathbf{r}'$  of counter-propagating paths is described by the propagator  $\Pi_C(\mathbf{r}, \mathbf{r}'; t)$ , the so-called Cooperon mode, which in the absence of decoherence obeys the same diffusion equation.

Let us now consider diffusive propagation in the presence of an external source of radiation, represented by a four-potential  $A = (\phi, \mathbf{a})$ , comprising a scalar and a vectorial component  $\phi = \phi(\mathbf{r}, t)$  and  $\mathbf{a} = \mathbf{a}(\mathbf{r}, t)$ , resp. To account for the externally imposed time dependence in a quantum diffusive process, we need to keep track of the traversal times of the participating Feynman paths. The situation is illustrated in Fig. 2. The left panel shows a diffuson mode comprising two amplitudes starting at times  $t^\pm - T$ , resp. and ending at  $t^\pm$ , where  $T$  is the time required to traverse the segment, and the dashed lines are symbolic for the quantum scattering events causing diffusion. The wiggly lines represent the action of the external field at time  $t^\pm - t$ . If the two paths are traversed simultaneously,  $t^+ = t^-$ , the potential affects the upper and lower line in the same way. In this case, the field does not destroy the mode, which is another way of saying that classical diffusion is not affected by quantum decoherence. The right panel shows the analogous situation for the Cooperon mode in a 'maximally crossed' representation of scattering events. The sign change in the time reversed potential  $TA = T(\phi, \mathbf{a}) = (\phi, -\mathbf{a})$  reflects the time reversal symmetry breaking nature of external vector potentials. Likewise, a time-dependent scalar potential  $\phi(t)$  will cause dephasing, unless an echo condition

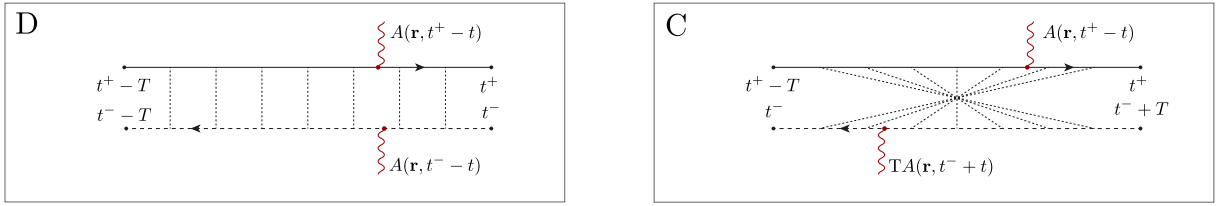


FIG. 2: Coupling of diffusion (left) and Cooperon (right) to an external field  $A = (\phi, \mathbf{a})$ . The field acts at position  $\mathbf{r}$  at the passage time of particle (upper line) and hole (lower line), respectively. If these positions differ, dephasing occurs. In the right panel,  $TA = T(\phi, \mathbf{a}) = (\phi, -\mathbf{a})$  indicates time reversal.

is met.

The influence of the field on the diffusion modes can be quantitatively described by diagrammatic perturbation theory [18]. Under the assumption that the external field is sufficiently weak not to change the classical trajectories but only alters the quantum phases, the perturbed diffusion and Cooperon modes ( $M = D, C$ ) are still governed by generalized diffusion equations

$$\begin{aligned} \mathcal{D}_M \Pi_M(\mathbf{r}, \mathbf{r}'; t^+, t^-, T) &= \delta(T) \delta(\mathbf{r} - \mathbf{r}'), \\ \mathcal{D}_{D/C} &= \partial_{t^+} \pm \partial_{t^-} - i[\phi(\mathbf{r}, t^+) - \phi(\mathbf{r}, t^-)] \\ &\quad - D (\partial_{\mathbf{r}} + i[\mathbf{a}(\mathbf{r}, t^+) \mp \mathbf{a}(\mathbf{r}, t^-)])^2, \end{aligned} \quad (3)$$

in which the field enters through a covariant derivative. For given  $A$ , these ‘imaginary-time Schrödinger equations’ can be solved, e.g., by path-integral techniques [18, 19]. We here consider a situation without magnetic field,  $\mathbf{a} = 0$ , and a scalar potential  $\phi(\mathbf{r}, t) = -\mathbf{r} \cdot \Delta \mathbf{p} f(t)$ ,  $f(t) = \hbar^{-1} \sum_{i=1}^N \delta(t - t_i)$  representing a spatially homogeneous force but temporally pulsed field. (The above weak field assumption requires that the momentum transferred by each pulse  $|\Delta \mathbf{p}| \ll p$  be much smaller than the particle momentum.) The time arguments relevant for the first-order quantum coherence contribution (1) are  $t^+ = t, t^- = 0, T = t$ , i.e. two counter-propagating paths running synchronously between time 0 and  $t$ . For times  $t < t_1$  before the first pulse the single Cooperon contribution  $X_{C1}(t) = c/(Dt)^{d/2}$  is just the classical probability of return within time  $t$ , where  $c$  is a numerical constant. The solution of the diffusion equation at times  $t > t_1$  exceeding the signal time is

$$\delta X_{C1}(t) = X_{C1}(t) e^{-|t-2t_1|/\tau_e}. \quad (4)$$

This result describes a near instantaneous destruction of the coherence contribution by the pulse at  $t_1$  followed by a revival at the echo time  $\tau_1 = 2t_1$  over a width  $\tau_e = \hbar^2/D\Delta p^2$ . To heuristically understand the echo profile, note that the phases of the two amplitudes are affected as  $\langle e^{i[\phi(\mathbf{r}(t_1)) - \phi(\mathbf{r}(T-t_1))]} \rangle \simeq e^{-\frac{1}{2} \langle [\phi(\mathbf{r}(t_1)) - \phi(\mathbf{r}(T-t_1))]^2 \rangle}$ , where the angular brackets represent averaging over path configurations. Substituting the potential and noting that for a diffusive process  $\langle [\mathbf{r}(t_1) - \mathbf{r}(t_2)]^2 \rangle \sim D|t_1 - t_2|$  one then obtains (4). The width of this echo is determined by the time scale  $\tau_e$  over which the phase mismatch

between the two amplitudes reaches unity,  $\langle (\Delta p \Delta x)^2 \rangle \sim \Delta p^2 D \tau_e = \hbar^2$ .

*Higher order quantum interference:*—The first-order coherence signal is suppressed after the C1 echo occurred at  $\tau_1$ . However, if a second pulse is applied at time  $t_2 > \tau_1$ , the coherence condition is met once more at  $\tau_2 \equiv t_1 + t_2$ , and another C1 echo will be observed [Fig. 1 c) second diagram]. In addition to this signal, however, the bi-temporal pulse gives rise to further echoes, and these probe quantum interference of more complex typography. Consider, for example, the D2 coherence process shown in figure Fig. 3, which describes the interference of co-propagating paths (no time reversal required!) along two loops which are traversed in different order. During its traversal of the upper loop, the particle is hit by the first pulse at time  $t_1$ . It then moves on into the second loop, where it is hit once more at  $t_2$ . A straightforward assignment of travel times to path segments shows that the hole amplitude (first going through the lower loop, then through the upper) will experience the pulses in synchronicity, i.e. at the same spatial path coordinates, provided the time of traversal for each loop equals  $t_2 - t_1$ . In this case, the process is coherent, and an echo will be observed at  $\tau_3 \equiv 2(t_2 - t_1)$ .

A similar argument shows that at the same time  $\tau_3$  the Cooperon process C2a shown in Fig. 3 – two counter-propagating loops traversed in the same order – becomes phase coherent, too. For that path configuration the coherence condition is satisfied at one more time,  $\tau_4 \equiv 2t_2 - t_1$  and this leads to one more echo C2b, also

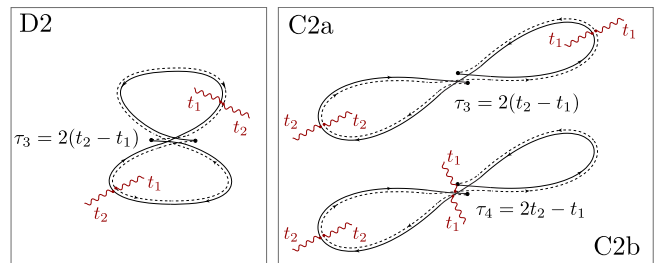


FIG. 3: Higher-order coherence contributions to the return amplitude probed by bi-temporal pulsing. Discussion, see text.

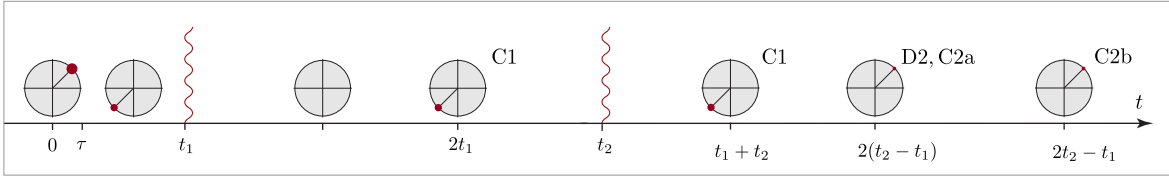


FIG. 4: Chronology of quantum coherence echoes in momentum space. Echoes are indicated by red dots whose width/angular orientation hint at the strength of the signal/orientation of the echo response in momentum space.

indicated in Fig. 3. A common feature of the processes D2, C2 is that they involve two diffusion modes, two diffusons (D2), or two Cooperons (C2). To quantitatively describe the echoes, we consider the solutions of the diffusion equations (3), for time arguments specified by the chronology of the corresponding path patterns. We obtain the echo contributions

$$\delta X_M(t) = X_M(t)e^{-|t-\tau_M|/\tau_e}, \quad M = \text{D2, C2a, C2b}, \quad (5)$$

where  $\tau_{\text{D2, C2a}} = \tau_3$ ,  $\tau_{\text{C2b}} = \tau_4$ , and  $X_M(t)$  are smoothly varying functions whose details are not relevant for the present discussion [20]. We note, however, that  $X_M$  is by a factor  $(E\tau/\hbar)^{1-d} \ll 1$  smaller than the strength function  $X_{\text{C1}}$  of the C1 process and that in this smallness reflects the relatively smaller phase volume available to the returning of higher-order path topologies. A typical chronology of echo signals is shown in Fig. 4, as a sequence of dots of varying strength and angular orientation. The latter refers to directional information encoded in momentum space correlation functions, as we are going to discuss next.

*Momentum space echoes:*—Although the essential classification of the system response in terms of echo times  $\{\tau_i\}$  and the corresponding path structures is universal, additional information can be obtained if observables different from the coordinate projectors  $\hat{O} = |\mathbf{r}\rangle\langle\mathbf{r}|$  are chosen. Specifically, we consider what happens if we turn to the complementary limit of momentum projectors,  $\hat{O} = |\mathbf{p}\rangle\langle\mathbf{p}|$ . A real space representation of Feynman paths describing classical scattering between generic states  $\mathbf{p} \rightarrow \mathbf{p}'$  is shown in the inset of Fig. 5 a), and the first coherence contribution, C1, in the main panel. The coherence of mutually time reversed paths connecting definite momenta does not require equality of the terminal real space coordinates, which is why C1 no longer assumes the form of a ‘loop’. It does, however, require opposite alignment of initial and final momentum,  $\mathbf{p}' = -\mathbf{p}$ . In a momentum resolved scattering experiment, the C1 echo would therefore be observed as a contribution to the backscattering probability, as indicated in Fig. 4. The lower panel of the figure exemplifies higher order quantum interference of momentum observables on the D2 process. As discussed above, D2 is formed by phase coherent superposition of two counter-propagating paths, and this requires alignment of initial

and final momenta,  $\mathbf{p}' = \mathbf{p}$ , i.e. the D2 process will contribute an echo at  $\tau_3$  in the *forward* scattering direction, which has been identified as particularly interesting [13] in connection with strong localization phenomena. The C2a and C2b processes are described by similar skeleton diagrams, but involve counter-propagating paths.

*Experimental realization and summary:*—We suggest to realize coherence echo spectroscopy in cold gases, where quantum interference of matter waves in random potential scattering has already been observed [15]. Here, a cloud of ultracold atoms is released as a Bose-Einstein condensate from a trap. The atoms are in a paramagnetic electronic ground state and suspended against gravity in a spatially homogeneous magnetic field gradient. By switching the magnetic field a well-defined initial wave packet can be prepared. A far-detuned optical speckle field then produces a conservative random potential in which the atomic cloud is let to evolve for some time before real-space [6] or momentum [15] distributions are measured. The key observation for our pro-

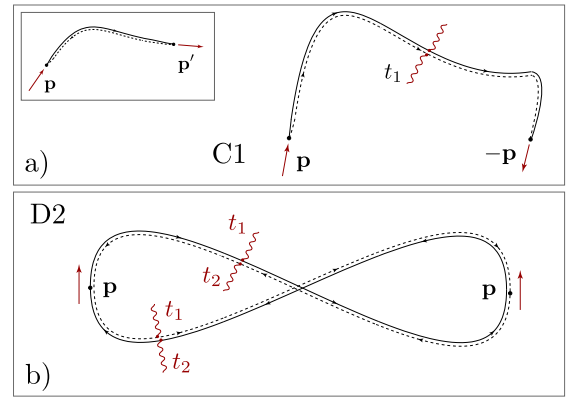


FIG. 5: Real space Feynman path representation of scattering probability between initial and final momentum states  $\mathbf{p}$  and  $\mathbf{p}'$ , resp. a) A singly pulsed Cooperon leads to a ‘coherent backscattering echo’ in direction  $\mathbf{p}' = -\mathbf{p}$ ; Inset: classical diffusion (immune against decoherence) between generic states  $\mathbf{p}$  and  $\mathbf{p}'$ . b) Two-mode coherent scattering under a bi-temporal pulse (here exemplified by the two-diffuson contribution) gives rise to echo signals in the forward-scattering direction  $\mathbf{p}' = \mathbf{p}$ .

posal is that the magnetic field gradient can be quickly switched to impart the proposed decoherence kicks during the diffusive propagation inside the disordered potential. A realization of the single-pulse scenario, therefore, seems immediately possible with the existing setup. The observation of the C1 echo would provide smoking gun evidence for the quantum mechanical coherence nature underlying the backscattering peak and exclude a classical origin [21, 22]. Observing higher order quantum interference signals may be experimentally challenging but is arguably realistic using similar setups, possibly constrained to lower-dimensional geometries. Such experiments would provide an unprecedented test of our understanding of those quantum mechanical coherence processes which eventually cause full Anderson localization of a wave packet in a disordered medium.

*Acknowledgements:*—T. M. gratefully acknowledges useful discussions with H. Micklitz and support by Brazilian agencies CNPq and FAPERJ. C.A.M. acknowledges hospitality of Université Pierre et Marie Curie and Laboratoire Kastler Brossel, Paris. A.A. acknowledges support by SFB/TR 12 of the Deutsche Forschungsgemeinschaft

- 
- [1] *50 Years of Anderson Localization*, E. Abrahams ed. (World Scientific, Singapore, 2010).
- [2] D. S. Wiersma, P. Bartolini, A. Lagendijk, R. Righini, Nature **390**, 671 (1997); T. Sperling, W. Bührer, C. M. Aegerter, and G. Maret, Nature Photon. **7**, 48 (2013).
- [3] A. A. Chabanov, M. Stoytchev, and A. Z. Genack, Nature **404**, 850 (2000).
- [4] P. W. Anderson, Phys. Rev. **109**, 1492 (1958).
- [5] J. Chabé, *et al.*, Phys. Rev. Lett. **101**, 255702 (2008).
- [6] J. Billy, V. Josse, Z. Zuo, A. Bernard, B. Hambrecht, P. Lugan, D. Clément, L. Sanchez-Palencia, P. Bouyer and A. Aspect, Nature **453**, 891 (2008).
- [7] G. Roati, C. D’Errico, L. Fallani, M. Fattori, C. Fort, M. Zaccanti, G. Modugno, M. Modugno, M. Inguscio, Nature **453**, 895 (2008).
- [8] S. S. Kondov, W. R. McGehee, J. J. Zirbel, B. DeMarco, Science **334**, 66 (2011).
- [9] T. Schwartz, G. Bartal, S. Fishman, M. Segev, Nature **446**, 52 (2007); Y. Lahini, A. Avidan, F. Pozzi, M. Sorel, R. Morandotti, D. N. Christodoulides, and Y. Silberberg Phys. Rev. Lett. **100**, 013906 (2008).
- [10] H. Hu, A. Strybulevych, J. H. Page, S. E. Skipetrov, B. A. van Tiggelen, Nat. Phys. **4**, 945 (2008).
- [11] E. Akkermans and G. Montambaux, *Mesoscopic Physics of Electrons and Photons* (Cambridge Univ. Press, 2006).
- [12] T. Karpiuk, N. Cherroret, K. L. Lee, B. Grémaud, C. A. Müller, C. Miniatura, Phys. Rev. Lett. **109**, 190601 (2012).
- [13] T. Micklitz, C. A. Müller, A. Altland, Phys. Rev. Lett. **112**, 110602 (2014).
- [14] N. Cherroret, T. Karpiuk, C. A. Müller, B. Grémaud, and C. Miniatura, Phys. Rev. A **85**, 011604(R) (2012).
- [15] F. Jendrzejewski, K. Müller, J. Richard, A. Date, T. Plisson, P. Bouyer, A. Aspect, V. Josse, Phys. Rev. Lett. **109**, 195302 (2012).
- [16] Comparison with the inset in Fig. 1a) suggests an interpretation of this ‘coherent backscattering amplitude’ as a weak localization process in pristine form, i.e. without external classical diffusion attached.
- [17] Another way of stating the same fact emphasizes the time reversal symmetry essential to the coherent backscattering signal: at time  $\tau_1 = 2t_1$ , time reversal  $t \rightarrow 2t_1 - t$  relative to the signal time  $t_1$  is restored and the conditions for phase coherence apply.
- [18] B. L. Altshuler, A. G. Aronov, *Electron-Electron Interaction in Disordered Systems* (Eds. A. L. Efros, M. Pollak), pp. 1-153 North-Holland, Amsterdam (1985).
- [19] R. P. Feynman and A. R. Hibbs, *Quantum Mechanics and Path Integrals*, (New York: McGraw-Hill 1965).
- [20] T. Micklitz, C. A. Müller, A. Altland, to be published.
- [21] G. Labeyrie, T. Karpiuk, J.-F. Schaff, B. Grémaud, C. Miniatura, D. Delande, Europhys. Lett. **100**, 66001 (2012).
- [22] N. Cherroret and D. Delande, Phys. Rev. A, **88**, 035602 (2013).